J|A|C|S
ARTICLES

Published on Web 12/31/2009

Hydrophobic Peptide Channels and Encapsulated Water Wires

Upadhyayula S. Raghavender,[†] Kantharaju,[‡] Subrayashastry Aravinda,[†] Narayanaswamy Shamala,*[,†] and Padmanabhan Balaram*[,‡]

Department of Physics and Molecular Biophysics Unit, Indian Institute of Science, Bangalore 560012, India

Received October 2, 2009; E-mail: shamala@physics.iisc.ernet.in; pb@mbu.iisc.ernet.in

Abstract: Peptide nanotubes with filled and empty pores and close-packed structures are formed in closely related pentapeptides. Enantiomorphic sequences, Boc-^{D}Pro-Aib-Xxx-Aib-Val-OMe (Xxx = Leu, **1**; Val, **2**; Ala, **3**; Phe, **4**) and Boc-Pro-Aib-^{D}Xxx-Aib-^{D}Val-OMe (^{D}Xxx = ^{D}Leu, **5**; ^{D}Val, **6**; ^{D}Ala, **7**; ^{D}Phe, **8**), yield molecular structures with a very similar backbone conformation but varied packing patterns in crystals. Peptides **1**, **2**, **5**, and **6** show tubular structures with the molecules self-assembling along the crystallographic six-fold axis (*c*-axis) and revealing a honeycomb arrangement laterally (*ab* plane). Two forms of entrapped water wires have been characterized in **2**: **2a** with $d_{O\cdots O} = 2.6$ Å and **2b** with $d_{O\cdots O} = 3.5$ Å. The latter is observed in **6** (**6a**) also. A polymorphic form of **6** (**6b**), grown from a solution of methanol−water, was observed to crystallize in a monoclinic system as a close-packed structure. Single-file water wire arrangements encapsulated inside hydrophobic channels formed by peptide nanotubes could be established by modeling the published structures in the cases of a cyclic peptide and a dipeptide. In all the entrapped water wires, each water molecule is involved in a hydrogen bond with a previous and succeeding water molecule. The O−H group of the water not involved in any hydrogen bond does not seem to be involved in an energetically significant interaction with the nanotube interior, a general feature of the one-dimensional water wires encapsulated in hydrophobic environements. Water wires in hydrophobic channels are contrasted with the single-file arrangements in amphipathic channels formed by aquaporins.

Introduction

Tubular structures are formed from both cyclic and acyclic peptides in the solid state. The original observation of a hybrid cyclic peptide stacking into a cylindrical structure by Karle et al.[1] was followed nearly two decades later by the elegant work of Ghadiri and co-workers on cyclic peptides, demonstrating nanotube formation in a cyclic sequence, cyclo-[^{D}Ala-Glu-^{D}Ala-Gln_2-], containing amino acid residues with alternating chirality.[2] Subsequent work established the ability of analogous sequences to form tubular structures.[3] More recently, Gorbitz has developed a class of dipeptides with hydrophobic side chains which form tubular structures in the solid state.[4] The recent interest in crystal structures that contain pores with molecular dimensions of 8−10 Å stems from their ability to serve as mimics for biological structures that are involved in transmembrane transport of small molecules and ions. Porous organic structures have also attracted considerable attention because of their potential in the areas of separation science, adsorption, and catalysis.[5] The selectivity of pores in organic solid-state structures is defined by the inner dimensions of the tube and the chemical nature of the groups that line the interior of the pore. As demonstrated by the work of the groups of Ghadiri and Gorbitz, peptides provide an excellent scaffold for the creation of tubular structures.

In the course of studies aimed at delineating the structure-directing properties of ^{D}Pro residues, we serendipitously encountered the formation of a tubular structure in the pentapeptide Boc-^{D}Pro-Aib-Leu-Aib-Val-OMe (**1**).[6] The peptide adopts a folded conformation stabilized by three intramolecular hydrogen bonds. The ^{D}Pro(1)-Aib(2) segment forms a Type II′ β-turn, while the Aib(2)-Aib(4) segment folds into a short stretch of a

[†] Department of Physics.
[‡] Molecular Biophysics Unit.

(1) Karle, I. L.; Handa, B. K.; Hassall, C. H. *Acta Crystallogr., Sect. B* **1975**, *31*, 555–560.
(2) Ghadiri, M. R.; Granja, J. R.; Milligan, R. A.; McRee, D. E.; Khazanovich, N. *Nature* **1993**, *366*, 324–327.
(3) (a) Ghadiri, M. R.; Granja, J. R.; Buehler, L. K. *Nature* **1994**, *369*, 301–304. (b) Khazanovich, N.; Granja, J. R.; McRee, D. E.; Milligan, R. A.; Ghadiri, M. R. *J. Am. Chem. Soc.* **1994**, *116*, 6011–6012. (c) Ghadiri, M. R.; Kobayashi, K.; Granja, J. R.; Chadha, R. K.; McRee, D. E. *Angew. Chem., Int. Ed. Engl.* **1995**, *34*, 93–95. (d) Engels, M.; Bashford, D.; Ghadiri, M. R. *J. Am. Chem. Soc.* **1995**, *117*, 9151–9158. (e) Clark, T. D.; Buehler, L. K.; Ghadiri, M. R. *J. Am. Chem. Soc.* **1998**, *120*, 651–656. (f) Bong, D. T.; Clark, T. D.; Granja, J. R.; Reza Ghadiri, M. *Angew. Chem., Int. Ed.* **2001**, *40*, 988–1011. (g) Bong, D. T.; Ghadiri, M. R. *Angew. Chem., Int. Ed.* **2001**, *40*, 2163–2166. (h) Fernandez-Lopez, S.; Kim, H.-S.; Choi, E. C.; Delgado, M.; Granja, J. R.; Khasanov, A.; Kraehenbuehl, K.; Long, G.; Weinberger, D. A.; Wilcoxen, K. M.; Ghadiri, M. R. *Nature* **2001**, *412*, 452–455. (i) Sanchez-Quesada, J.; Isler, M. P.; Ghadiri, M. R. *J. Am. Chem. Soc.* **2002**, *124*, 10004–10005. (j) Horne, W. S.; Stout, C. D.; Ghadiri, M. R. *J. Am. Chem. Soc.* **2003**, *125*, 9372–9376.
(4) (a) Gorbitz, C. H.; Gundersen, E. *Acta Crystallogr., Sect. C* **1996**, *52*, 1764–1767. (b) Gorbitz, C. H. *Chem.—Eur. J.* **2001**, *7*, 5153–5159. (c) Gorbitz, C. H. *New J. Chem.* **2003**, *27*, 1789–1793. (d) Gorbitz, C. H. *Chem.—Eur. J.* **2007**, *13*, 1022–1031. (e) Gorbitz, C. H.; Rise, F. *J. Pept. Sci.* **2008**, *14*, 210–216.
(5) (a) Kitagawa, S.; Kitaura, R.; Noro, S.-I. *Angew. Chem., Int. Ed.* **2004**, *43*, 2334–2375. (b) Scanlon, S.; Aggeli, A. *Nano Today* **2008**, *3*, 22–30. (c) Bonifazi, D.; Mohnani, S.; Llanes-Pallas, A. *Chem.—Eur. J.* **2009**, *15*, 7004–7025. (d) Yang, Z.; Lu, Y.; Yang, Z. *Chem. Commun.* **2009**, *17*, 2270–2277.
(6) Raghavender, U. S.; Aravinda, S.; Shamala, N.; Kantharaju; Rai, R. K.; Balaram, P. *J. Am. Chem. Soc.* **2009**, *131*, 15130–15132.

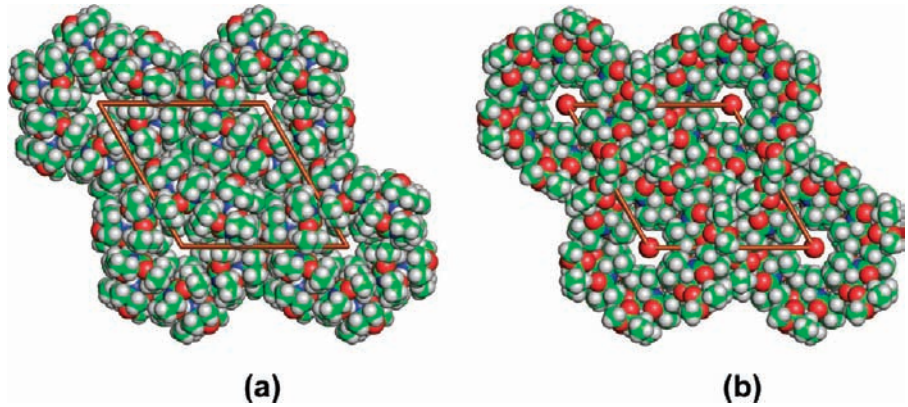

Figure 1. Crystal lattice (honeycomb pattern) of linear, acyclic, hydrophobic pentapeptides **1** (left, Xxx = Leu) and **2a** (right, Xxx = Val), revealing a two-dimensional array of nanotubes (projection down *c*-axis). (a) Peptide **1** shows hollow tubes (diameter ~5.2 Å). (b) Peptide **2a** shows water-filled channels (diameter ~7.5 Å).

right-handed 3_{10} helical structure. The molecule is then left with only one free amide NH group of Aib(2). In crystals, this lone NH group forms an intermolecular hydrogen bond to a peptide carbonyl, CO of Leu(3). The formation of crystals in the space group $P6_5$ reveals a helical array of peptides about the *c*-axis linked by a single hydrogen bond to their neighbors. This arrangement results in the formation of a hollow tube for the column of molecules arranged about the crystallographic six-fold axis (*c*-axis). Further assembly of these tubular structures results in a crystal lattice that contains a two-dimensional array of peptide nanotubes (Figure 1). The inner diameter of the pore, which is unoccupied, is ~5.2 Å. The inner lining is entirely hydrophobic, a property of the sequence, with the isobutyl groups of Leu(3) pointing into the pore. Modeling studies suggest that even water molecules cannot be accommodated in such a pore, as a result of severe short contacts with the atoms lining the inner walls. We therefore turned to a peptide with a shorter side chain at position 3, Boc-^{D}Pro-Aib-Val-Aib-Val-OMe (**2**), which also crystallized in the space group $P6_5$. Structure determination revealed a pore diameter of ~7.5 Å, with a one-dimensional wire of water molecules occupying the hollow tube (Figure 1). The crystal structure of **2** was determined for two crystal forms which differed only in the structures of water wires. Peptide **2** provides a well-characterized example of a one-dimensional array of water molecules connected by hydrogen bonds, with no significant stabilizing contacts with the surrounding walls of the encapsulating molecular tube.[6] In order to examine the role of residue 3 in generating peptide nanotubes, we synthesized the analogues Boc-^{D}Pro-Aib-Xxx-Aib-Val-OMe (Xxx = Ala, **3**; Phe, **4**). As part of a program to study the packing effects in peptide racemates, we examined the enantiomeric sequences, Boc-Pro-Aib-^{D}Xxx-Aib-^{D}Val-OMe (^{D}Xxx = ^{D}Leu, **5**; ^{D}Val, **6**; ^{D}Ala, **7**; ^{D}Phe, **8**). Peptides **5**−**8** also provided an opportunity to examine the crystal structures of the enantiomers of peptides **1**−**4**. In a previous study of diproline peptides, we have reported the utility of attempting to crystallize peptides and their enantiomers under a variety of conditions which facilitate the search for polymorphic forms.[7] In this report, we describe the structures of peptides **1**−**8**. Peptide **6**, Boc-Pro-Aib-^{D}Val-Aib-^{D}Val-OMe, provides an example of a situation where two polymorphic forms are characterized with one revealing a tubular structure while the other established a close-packed arrangement. The characterization of water wires in the crystal forms of **2** and **6** has also prompted us to examine models for water molecules in hydrophobic tubes formed by the cyclic peptides of Ghadiri and co-workers and the dipeptides of Gorbitz.[3d,4c] The results establish that hydrophobic tubes constructed from peptide scaffolds can provide a sequestering environment for one-dimensional water wires, permitting detailed structural characterization.

Single-file water wires that traverse hydrophobic channels are of special interest in building models for understanding proton and water translocation across biological membranes. The structural properties of ordered water arrays assume increasing significance in view of the growing recognition of the role of water in confined spaces which are routinely encountered in cellular phenomena.[8]

Results and Discussion

Molecular Conformation in Crystals. Ten independent crystal structures were determined for the peptide series Boc-^{D}Pro-Aib-Xxx-Aib-Val-OMe (**1**−**4**) and the enantiomeric series Boc-Pro-Aib-^{D}Xxx-Aib-^{D}Val-OMe (**5**−**8**). For peptides **2** (Xxx = ^{L}Val) and **6** (Xxx = ^{D}Val), two independent crystal forms were characterized. Forms **2a** and **2b** were very similar, differing only in the nature of the water incorporated into the pores formed in the hexagonal space group $P6_5$. In contrast, for peptide **6**, two distinct polymorphic forms were obtained. In **6a**, molecules pack into a hexagonal space group ($P6_1$) with a central pore, while **6b** is a close-packed form (space group *C*2). Relevant crystal and diffraction parameters are listed in Table 1. Figure 2 shows the molecular conformation for all the ten cases. Backbone dihedral angles are summarized in Table 2. In all cases, the peptide molecules adopt a folded conformation stabilized by three intramolecular 4→1 hydrogen bonds: Xxx(3) NH···OC, Boc(0) and Aib(4) NH···OC, ^{D}Pro(1) and Val(5) NH···OC for **1**−**4**; ^{D}Xxx(3) NH···OC, Boc(0) and Aib(4) NH···OC, and Pro(1) and ^{D}Val(5) NH···OC ^{D}Xxx(3) for **5**−**8** (see Table 2 footnotes and Supporting Information Tables S5 and S6 for details of hydrogen bond parameters). Figure 3 illustrates the superposition for the four structures in each enantiomeric set and also provides the Ramachandran plot for both sets of peptides. The backbone folding pattern for the pentapeptides may be classified as a Type II′ β-turn followed by a single right-handed 3_{10} helical turn (**1**−**4**) and a Type II β-turn followed by a left-handed 3_{10} helical turn (**5**−**8**). These crystallographic

(7) (a) Chatterjee, B.; Saha, I.; Raghothama, S.; Aravinda, S.; Rai, R.; Shamala, N.; Balaram, P. *Chem.—Eur. J.* **2008**, *14*, 6192–6204. (b) Saha, I.; Chatterjee, B.; Shamala, N.; Balaram, P. *Biopolymers (Peptide Sci.)* **2008**, *90*, 537–543.
(8) Ball, P. *Chem. Rev.* **2008**, *108*, 74–108.

Table 1. Crystal Parameters, Unit Cell Dimensions, and Final *R*-Factors for Peptides **1**−**8**

Boc-^{D}Pro-Aib-Xxx-Aib-Val-OMe					
	1	**2a**	**2b**	**3**	**4**
Xxx	Leu	Val	Val	Ala	Phe
empirical formula	$C_{30}H_{53}N_5O_8$	$C_{29}H_{51}N_5O_8$	$C_{29}H_{51}N_5O_8$	$C_{27}H_{47}N_5O_8$	$C_{33}H_{48}N_5O_8$
crystal size (mm^3)	0.4 × 0.21 × 0.03	0.45 × 0.12 × 0.07	0.45 × 0.12 × 0.07	0.45 × 0.29 × 0.20	0.60 × 0.38 × 0.39
crystallizing solvent	methanol/water	ethyl acetate/pet. ether	ethyl acetate/pet. ether	methanol/water	acetonitrile/water
space group	$P6_5$	$P6_5$	$P6_5$	$P2_12_12_1$	$P2_12_12_1$
a (Å)	24.3673(9)	24.2920(13)	24.3161(3)	12.2403(8)	10.3268(8)
b (Å)	24.3673(9)	24.2920(13)	24.3161(3)	15.7531(11)	18.7549(15)
c (Å)	10.6844(13)	10.4830(11)	10.4805(1)	16.6894(11)	18.9682(16)
V (Å^3)	5494.09(7)	5357.67(7)	5366.62(1)	3218.09(4)	3673.73(5)
final *R* (%)	6.37	5.5	6.2	4.4	4.7
final wR_2 (%)	14.5	15.5	18.4	12.5	13.2

Boc-Pro-Aib-^{D}Xxx-Aib-^{D}Val-OMe					
	5	**6a**	**6b**	**7**	**8**
^{D}Xxx	^{D}Leu	^{D}Val	^{D}Val	^{D}Ala	^{D}Phe
empirical formula	$C_{30}H_{53}N_5O_8$	$C_{29}H_{51}N_5O_8$	$C_{29}H_{51}N_5O_8$	$C_{27}H_{47}N_5O_8$	$C_{33}H_{48}N_5O_8$
crystal size	0.6 × 0.4 × 0.16	0.56 × 0.10 × 0.04	0.75 × 0.01 × 0.19	0.34 × 0.18 × 0.14	0.51 × 0.29 × 0.42
crystallizing solvent	dioxane/water	ethyl acetate/pet. ether	methanol/water	methanol/water	dioxane/water
space group	$P6_1$	$P6_1$	$C2$	$P2_12_12_1$	$P2_12_12_1$
a (Å)	24.4102(8)	24.3645(14)	20.7278(35)	12.2528(12)	10.3354(5)
b (Å)	24.4102(8)	24.3645(14)	9.1079(15)	15.7498(16)	18.7733(10)
c (Å)	10.6627(7)	10.4875(14)	19.5728(33)	16.6866(16)	18.9820(10)
β (°)			94.207(3)		
V (Å^3)	5502.3(4)	5391.60(8)	3685.1(11)	3220.2(5)	3683.1(3)
final *R* (%)	5.4	7.5	6.6	4.7	5.1
final wR_2 (%)	14.9	18.1	17.6	12.8	15.3

observations establish the robustness of the backbone conformation adopted by the pentapeptide sequences, in which structural rigidity is conferred by the N-terminus ^{D}Pro/^{L}Pro-Aib segment and Aib residue at position 4. The role of the residue at position 3 in determining packing in crystals can therefore be investigated.

Packing in Crystals. Peptide enantiomers **1** and **5** crystallize in the space groups $P6_5$ and $P6_1$, respectively, as illustrated in Figure 4. Neighboring molecules are linked by a single intermolecular hydrogen bond (Aib(2)NH···OC Val(3)), forming a superhelix about the six-fold axis, resulting in a central hollow tube, decorated with the methyl groups of the Boc protecting group and the leucine side chain. The tubular peptide structures assemble into a two-dimensional array. The central pore has a diameter of ∼5.2 Å, estimated by the procedure proposed by Miyazawa.[9] Peptide **6** (Xxx = ^{D}Val) crystallizes in two distinct polymorphic forms. Form **6a**, illustrated in Figure 5, displays a packing arrangement almost identical to that observed in **1**, **2**, and **5**. The shortening of the side chain at position 3 results in expanding the diameter of the tubular peptide structures to ∼7.6 Å. As in the case of the enantiomeric peptide **2**, water molecules are identifiable in the hydrophobic channel forming a one-dimensional water wire, which will be considered later. Interestingly, in the polymorphic form **6b**, peptide molecules crystallize in a close-packed arrangement in the monoclinic space group *C*2, with two water molecules (full occupancy), which form bridges between symmetry-related molecules. A further reduction of the size of the residue at position 3 in peptides **3** (Xxx = Ala) and **7** (^{D}Xxx = ^{D}Ala) results in close-packed structures in the space group $P2_12_12_1$, with no solvent molecules (Figure 5). The introduction of a bulky aromatic side chain at position 3 in peptides **4** (Xxx = Phe) and **8** (^{D}Xxx = ^{D}Phe) results in the formation of crystals in the space group $P2_12_12_1$. Here the molecules are close-packed and there is no co-crystallized solvent. Symmetry-related peptide molecules also show evidence of a significant aromatic−aromatic interaction between projecting Phe residues (Figure 6).[10]

The 10 crystal structures determined for peptides **1**−**8** establish that peptide nanotube formation is critically determined by the size of the side chain at position 3. Tubular structures could be demonstrated when Xxx = Leu/Val in both the enantiomeric series. Packing into hexagonal space groups $P6_1$ and $P6_5$ permits the formation of a hydrophobic channel which runs through the crystal along the six-fold axis, with the side-chain atoms of residue 3 projecting inward. The solvent occupancy of the channel depends on the steric bulk of the side chains. In the case of Leu residues, the size of the isobutyl group reduced the diameter of the channel to ∼5.2 Å, precluding the entry of even water molecules. Despite the presence of empty pores which run through the lattice, this packing arrangement appears to be stable in crystals, being observed in both peptides **1** and **5**. In contrast, peptides **2** and **6**, which possess the smaller valine side chain, show evidence for both solvent-filled hydrophobic channels and close-packed polymorphs, which lack the pores running through the crystal. The observation suggests that the presence of hydrophobic channels with diameter significantly greater than 5.5 Å may be unstable unless occupied by solvent. The formation of both porous and close-packed polymorphs should then be determined by the kinetics of nucleation of the crystal. If a very small side chain is placed at position 3, as in the case of peptides **3** (Xxx = Ala) and **7** (^{D}Xxx = ^{D}Ala), the anticipated pore size should be ∼10 Å. Formation of such a large diameter channel would tend to be energetically unfavorable when compared to the observed close-packed structure. As anticipated, the bulky side chain at position 3 precludes the

(9) Miyazawa, T. *J. Polym. Sci.* **1961**, *55*, 215–231.

(10) Aravinda, S.; Shamala, N.; Das, C.; Sriranjini, A.; Karle, I. L.; Balaram, P. *J. Am. Chem. Soc.* **2003**, *125*, 5308–5315.

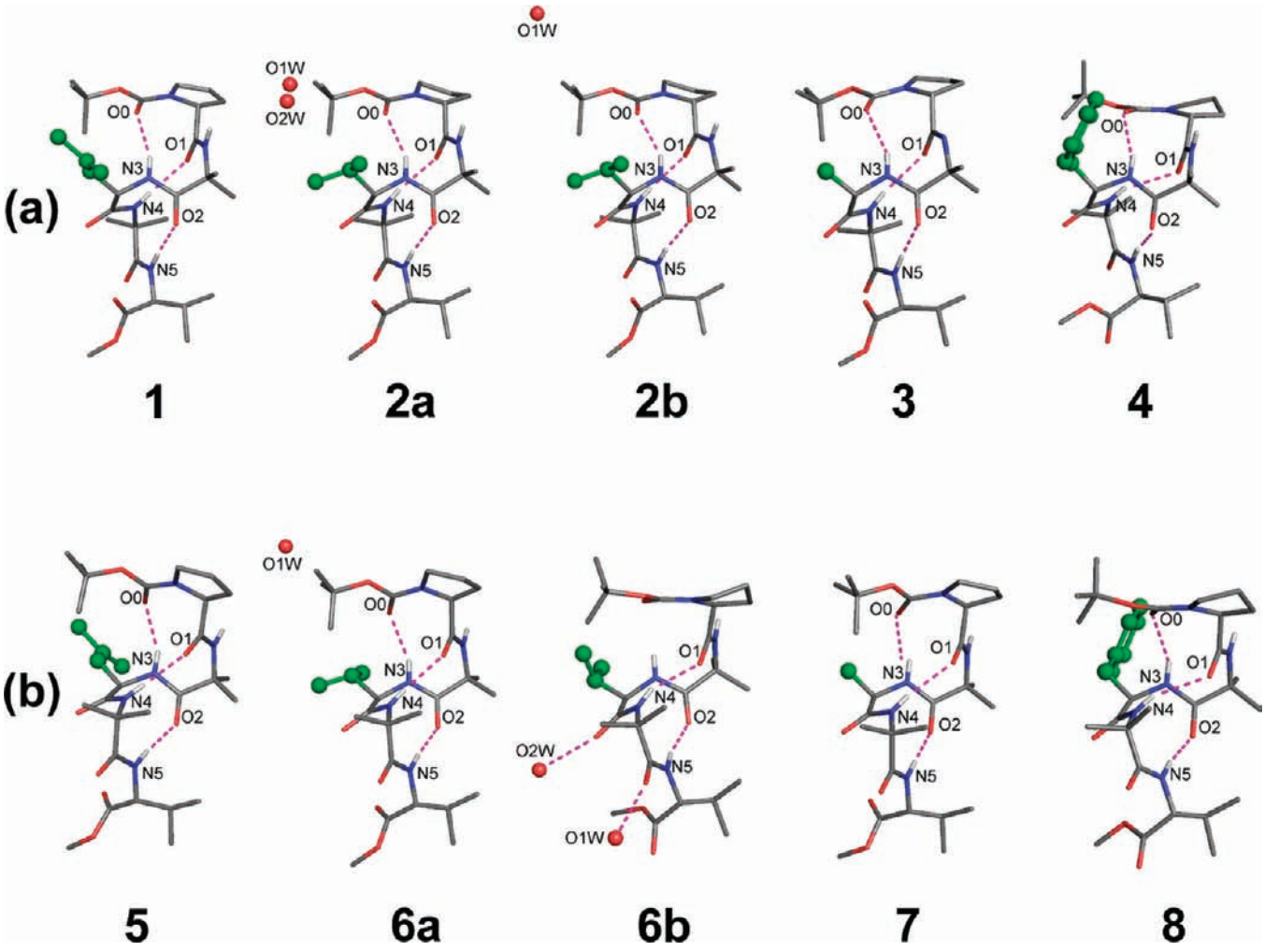

Figure 2. Molecular conformation and the asymmetric unit of the peptides (a) Boc-^{D}Pro-Aib-Xxx-Aib-Val-OMe (Xxx = Leu, **1**; Val, **2a/2b**; Ala, **3**; Phe, **4**) and (b) Boc-Pro-Aib-^{D}Xxx-Aib-^{D}Val-OMe (^{D}Xxx = ^{D}Leu, **5**; ^{D}Val, **6a/6b**; ^{D}Ala, **7**; ^{D}Phe, **8**). Xxx residues are shown as spheres (green). Intramolecular 4→1 hydrogen bonds are shown as dashed lines.

Table 2. Backbone Torsion Angles for Peptides **1**−**8**[a]

Boc-^{D}Pro-Aib-Xxx-Aib-Val-OMe

	1 Xxx = Leu			**2a** Xxx = Val			**2b** Xxx = Val			**3** Xxx = Ala			**4** Xxx = Phe		
	ϕ	ψ	ω	ϕ	ψ	ω	ϕ	ψ	ω	ϕ	ψ	ω	ϕ	ψ	ω
^{D}Pro(1)	51.6	−134.1	−174.1	52.9	−136.6	−174.0	53.9	−137.0	−174.2	55.1	−146.7	−175.4	61.4	−139.8	−176.7
Aib(2)	−57.9	−24.2	−177.9	−59.3	−24.7	−177.8	−59.6	−24.2	−178.0	−61.8	−20.8	−178.6	−54.6	−35.5	−170.6
Xxx(3)	−72.7	−1.1	165.7	−73.6	−1.2	162.6	−73.9	−1.2	162.4	−68.7	−8.8	167.2	−70.8	−17.9	178.4
Aib(4)	−57.3	−29.3	−177.3	−55.5	−32.0	−175.6	−55.4	−31.6	−175.7	−54.4	−31.0	−177.5	−71.2	−16.9	178.4
Val(5)	−90.1	133.3	176.5	−85.3	130.2	175.7	−85.7	130.3	175.8	−93.0	135.0	178.9	−68.2	−42.4	179.6

Boc-Pro-Aib-^{D}Xxx-Aib-^{D}Val-OMe

	5 ^{D}Xxx = ^{D}Leu			**6a** ^{D}Xxx = ^{D}Val			**6b** ^{D}Xxx = ^{D}Val			**7** ^{D}Xxx = ^{D}Ala			**8** ^{D}Xxx = ^{D}Phe		
	ϕ	ψ	ω	ϕ	ψ	ω	ϕ	ψ	ω	ϕ	ψ	ω	ϕ	ψ	ω
Pro(1)	−50.5	133.5	173.9	−52.5	136.5	174.1	−63.3	151.8	170.5	−55.1	146.7	175.2	−61.4	139.8	176.4
Aib(2)	58.6	22.9	179.2	58.9	24.9	177.5	47.6	46.5	168.9	61.8	20.7	178.8	54.8	35.3	170.6
^{D}Xxx(3)	73.2	0.4	−165.4	73.5	1.2	−163.0	73.7	7.2	−169.7	68.9	8.5	−167.3	71.0	17.4	−178.2
Aib(4)	56.7	31.8	176.1	55.2	32.6	175.5	63.3	18.9	178.6	54.7	30.7	177.6	71.6	16.5	−178.3
^{D}Val(5)	87.5	−132.9	−175.8	84.5	−130.5	−176.4	91.0	48.7	−167.6	93.1	−134.8	−179.0	68.7	43.3	177.7

[a] Mean values for hydrogen bond parameters for peptides **1**−**4**: intramolecular hydrogen bonds, N···O = 3.111 Å, H···O = 2.314 Å, ∠N−H···O = 157.35°; intermolecular hydrogen bonds, N···O = 2.942 Å, H···O = 2.094 Å, ∠N−H···O = 167.54°. Mean values for hydrogen bond parameters for peptides **5**−**8**: intramolecular hydrogen bonds, N···O = 3.079 Å, H···O = 2.283 Å, ∠N−H···O = 157.91°; intermolecular hydrogen bonds, N···O = 2.976 Å, H···O = 2.134 Å, ∠O = 166.53°.

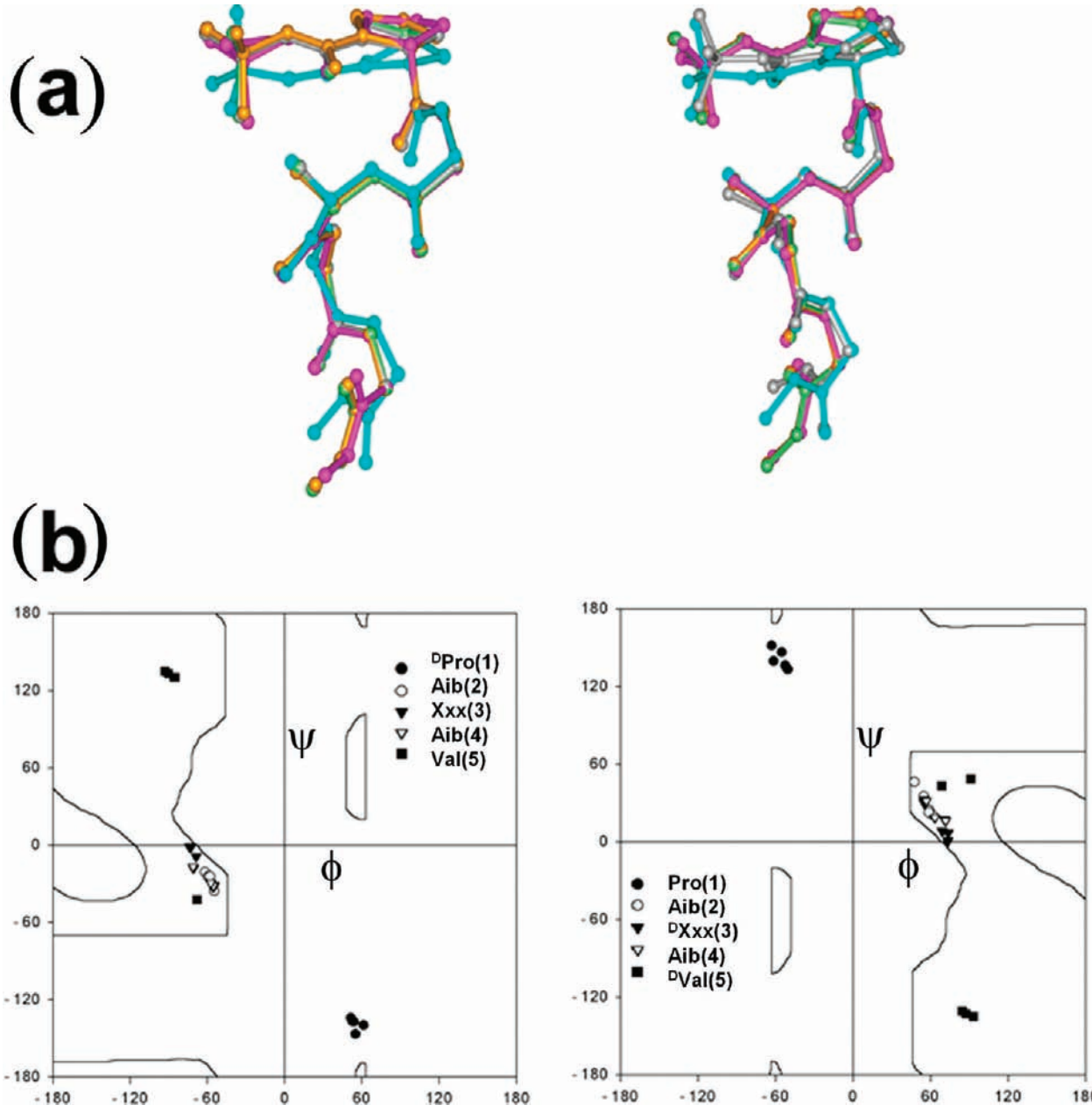

Figure 3. (a) Superposition of the backbone atoms (N, C^{α}, C, O) and β-carbon of Xxx residues in the pentapeptides **1**−**4** (rmsd = 0.18 Å) and **5**−**8** (rmsd = 0.25 Å). (b) Ramachandran plots indicating the backbone torsion angles adopted by the peptides **1**−**4** and **5**−**8**.

formation of a tubular structure, as demonstrated for peptides **4** (Xxx = Phe) and **8** (^{D}Xxx = ^{D}Phe).

Water Wires in Hydrophobic Channels. In the pentapeptide series, Boc-^{D}Pro-Aib-Xxx-Aib-Val-OMe, and the enantiomeric series, Boc-Pro-Aib-^{D}Xxx-Aib-^{D}Val-OMe, the independent crystal structure determinations of peptides **2a**/**2b** (Xxx = Val) and **6a** (^{D}Xxx = ^{D}Val) provide a direct observation of one-dimensional arrays of water molecules. In all three cases, the tubular channel running through the crystal is occupied by water molecules. Refinements of the crystal structures lead to partial occupancies of oxygen atoms at sites along the six-fold axis. Inspection of O···O distances permits the building of a water wire model which is stereochemically acceptable, with no short O···O contacts. In **2a**, water molecules arranged along the six-fold axis are separated by an O···O distance of 2.6 Å, while in **2b** the O···O separation is 3.5 Å. The crystal structure of **2b** was obtained after the crystal of **2a** was stored at room temperature for several weeks. The *c*-axis dimension (∼10.48 Å) in the hexagonal unit cell results in four water molecules in the unit cell (six peptides) for **2a**, while in **2b** there are three water molecules. In the derived water wire models each water makes two hydrogen bond contacts, one donor and one acceptor, to near neighbors (water molecules). The second O−H bond of the water molecule points toward the hydrophobic wall of the channel. The range of H···H contacts between the water molecule and the channel walls is 2.9−4.9 Å, suggesting that the interactions between the embedded water wire and the surrounding hydrophobic tube must be extremely weak. Water molecules can execute a rotational motion about the six-fold axis (hydrogen bond direction), contributing entropically to the net free energy of stabilization of the observed structure.[6] The crystal structure of peptide **6a** (^{D}Xxx = ^{D}Val) and the geometry of the water wire are identical to those observed in **2b** (Figure 7a).

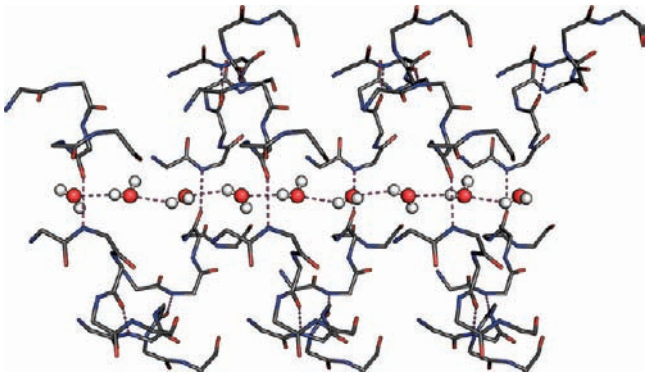

Figure 4. Encapsulated water wire in the peptide **6a**, Boc-Pro-Aib-^{D}Val-Aib-^{D}Val-OMe. The peptide backbone is shown as sticks, and the water molecules are shown as spheres. The lone intermolecular hydrogen bond between the peptide molecules and the water−water hydrogen bonds are shown as dashed lines.

The unexpected characterization of the water wires in the hydrophobic channels formed by the linear, protected, apolar pentapeptides prompted us to re-examine the nature of the solvent structure in the previously reported peptide nanotubes. The work of Ghadiri and co-workers established that cyclic octapeptides containing alternating L,D residues formed disc-like structures, which self-assemble to form tubular arrays.[3] In these molecules the peptide bonds are approximately parallel to the long axis of the nanotube, with the amino acid side chains projecting outward. Stacking of disc-like peptides is facilitated by multiple hydrogen-bonding interactions between neighboring molecules in the peptide cyclo-[(Phe-^{D,Me}NAla)$_4$-], with an internal tube diameter of ∼10 Å. Ghadiri et al. noted, "The tubular cavity is filled with partially disordered water molecules". They added, "water molecules near the hydrophobic domains are considerably more disordered, displaying only a weak residual electron density. The observed electron density for water is the time-average of water molecules binding at several overlapping sites, which suggests a facile movement of loosely held water molecules within the cavity." [3c] In the reported structure, the peptide crystallized in the space group *I*422 with one molecule in the asymmetric unit. The deposited coordinates for five water molecules lead to the O···O separations shown in Figure 8a. It may be noted that four water molecules, Ow1 to Ow4, are arranged in a linear fashion with O···O separations of 1.58−1.67 Å. A significantly larger separation of 5.12 Å is observed between Ow4 and Ow5. In this model, the water molecule Ow5 would appear to be isolated, lacking either donor or acceptor for hydrogen bond interactions. The immediate environment of Ow5 reveals a cluster of phenyl rings from symmetry-related molecules which surround the water molecule. The observed distances between the oxygen atom and the nearest atom of the phenyl rings lie between 4.6 and 5.0 Å, suggesting the absence of any appreciable non-covalent interactions involving this lone water molecule (Figure 8b). This led to the consideration of an alternate model for the single-file water molecules encapsulated within the hydrophobic channels formed by the assembly of the cyclic peptide. Insertion of two additional oxygen atoms between Ow4 and Ow5 leads to the arrangement shown in Figure 8c. In this model, the O···O distances between the water molecules are completely disallowed sterically. The stereochemically acceptable distances may therefore be derived by considering alternate water molecules along the axis of the hydrophobic channel. This arrangement is illustrated in Figure 8d. The O···O distances between the adjacent water molecules is now ∼3.2 Å, and each water molecule is involved in two hydrogen bond interactions (one donor/one acceptor) with near neighbors. The resulting water wire structure is almost identical to that described above for peptides **2a**, **2b**, and **6a**. Re-examination of the electron density for the entrapped water molecules may provide some further insights.

Dipeptides with free amino and carboxylic acid groups have been shown by Gorbitz to crystallize in hexagonal space groups, incorporating tubular channels which run through the crystal.[4] The dipeptide Val-Ile yielded crystals in the space group $P6_1$ with one molecule in the asymmetric unit. Crystal structure solution using low-temperature data (T = 105 K) revealed a co-crystallized water molecule, disordered over two sites, with partial occupancies of 0.24 and 0.14.[4c] Interestingly, the distance between the two disordered water molecules is 0.9 Å, with the *c*-axis dimension of ∼10.314 Å, corresponding to the repeat spacing about the six-fold axis. This length (*c*-axis) corresponds closely to the *c*-axis dimension of the pentapeptides **2a**, **2b**, and **6a**.[6] A water wire can therefore be modeled along the *c*-axis, which satisfies the steric criteria for adjacent molecules. The resultant model yields four water molecules in the unit cell (Figure 9). Inspection of the water environment establishes that the walls of the nanotube formed by the dipeptides are composed exclusively of the isopropyl side chains of Val residues. The distance between the oxygen atoms of the water molecules and the hydrogen atoms lining the tube interior lies between 2.97 and 3.71 Å. As in the case of **2a**, **2b**, and **6a**, the water molecules occupy unique environments. The symmetry of the space group is not manifested in the water wires within the hydrophobic nanotubes of the peptide crystals. The resultant peptide stoichiometry would then be six peptide/four water molecules.

One-dimensional arrays of water molecules ("wires") are also involved in the single-file transport of water through the aquaporins.[11] Elegant biochemical and crystallographic work on aquaporins, which form water-permeable channels across biological membranes, has revealed an architecture which may be compared with the hydrophobic peptide channels described above.[11] Figure 10 illustrates the water wire characterized in the crystal structure of the human aquaporin 4 (AQP4).[11e] The O···O distances between hydrogen-bonded pairs are 2.31−2.96 Å, very close to that observed in peptide **2a**. In the case of aquaporins, one face of the tubular channel is lined by hydrophobic side chains of Val, Leu, and Ile residues, while the other face is composed of polar groups which can hydrogen bond to the water molecules. The distances between the water oxygen atoms and the apolar methyl groups which are closest to the waters range 3.65−4.84 Å, very close to those observed in the hydrophobic peptide nanotubes. The amphipathic nature of the lining of the APQ4 channel may be of some relevance in precluding proton transport while facilitating the perme-

(11) (a) Fujiyoshi, Y.; Mitsuoka, K.; De Groot, B. L.; Philippsen, A.; Grubmuller, H.; Agre, P.; Engel, A. *Curr. Opin. Struct. Biol.* **2002**, *12*, 509–515. (b) Engel, A.; Nielsen, S. *J. Physiol.* **2002**, *542*, 3–16. (c) Nielsen, S.; Frokiaer, J.; Marples, D.; Kwon, T.-H.; Agre, P.; Knepper, M. A. *Physiol. Rev.* **2002**, *82*, 205–244. (d) Khalili-Araghi, F.; Gumbart, J.; Wen, P. C.; Sotomayor, M.; Tajkhorshid, E.; Schulten, K. *Curr. Opin. Struct. Biol.* **2009**, *19*, 128–137. (e) Ho, J. D.; Yeh, R.; Sandstrom, A.; Chorny, I.; Harries, W. E. C.; Robbins, R. A.; Miercke, L. J. W.; Stroud, R. M. *Proc. Natl. Acad. Sci. U.S.A.* **2009**, *106*, 7437–7442.

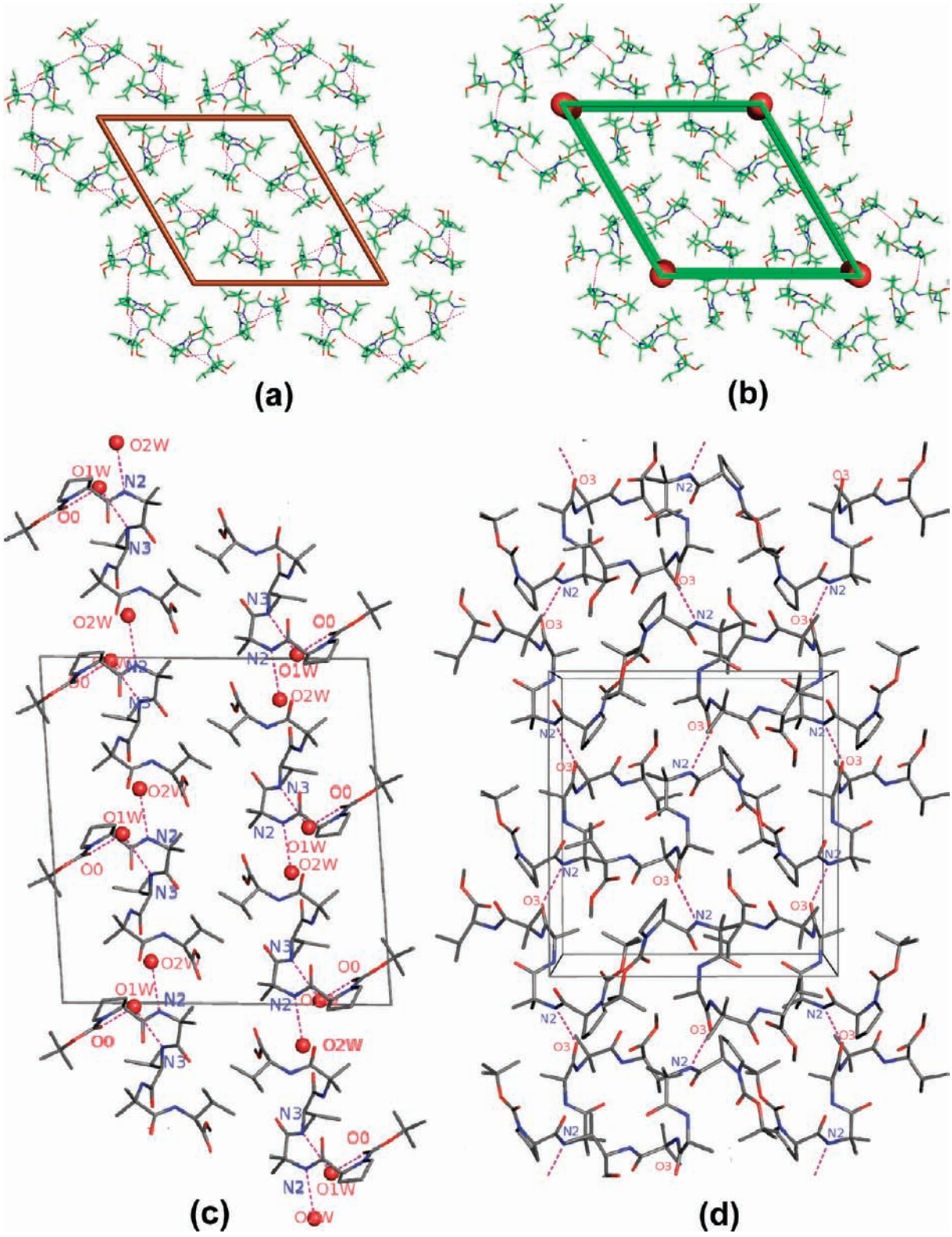

Figure 5. Molecular packing of the peptides in crystals: (a) **5** and (b) **6a**, viewed down the *c*-axis; (c) **6b**, viewed down the *b*-axis; and (d) **7**, viewed down the *a*-axis.

ation of neutral water molecules, a key feature of the biological function of the protein. It should be noted that rapid transport of protons by the Grotthuss mechanism would involve correlated rotation of the water molecule along the wire, resulting in shifts of the hydrogen-bonded protons.

The area of water and proton transport across biological membranes has been a subject of considerable interest in recent years.[12] The structure and dynamics of water molecules embedded in hydrophobic channels and carbon nanotubes has been extensively investigated by theoretical methods.[13] The ability

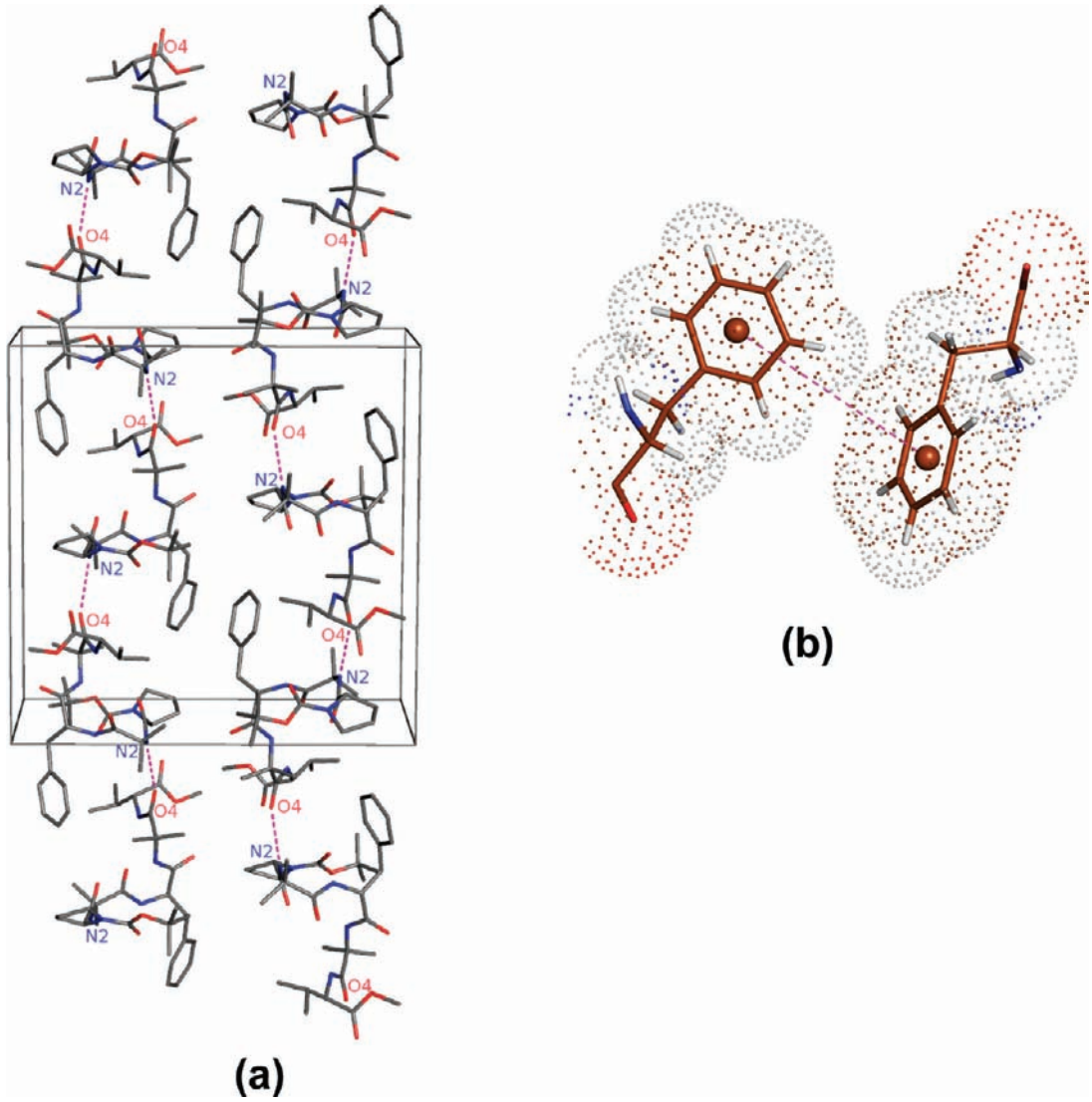

Figure 6. (a) Molecular packing of the peptide **8**, Boc-Pro-Aib-^{D}Phe-Aib-^{D}Val-OMe, viewed down the *a*-axis. (b) Aromatic−aromatic (^{D}Phe-^{D}Phe) interactions (see ref 10 for definition of parameters) in the peptide **8**: $R_{cen} = 6.05$ Å, $R_{clo} = 4.15$ Å, and $\gamma = 49.61°$. Centroid−centroid distance is shown as dashed line.

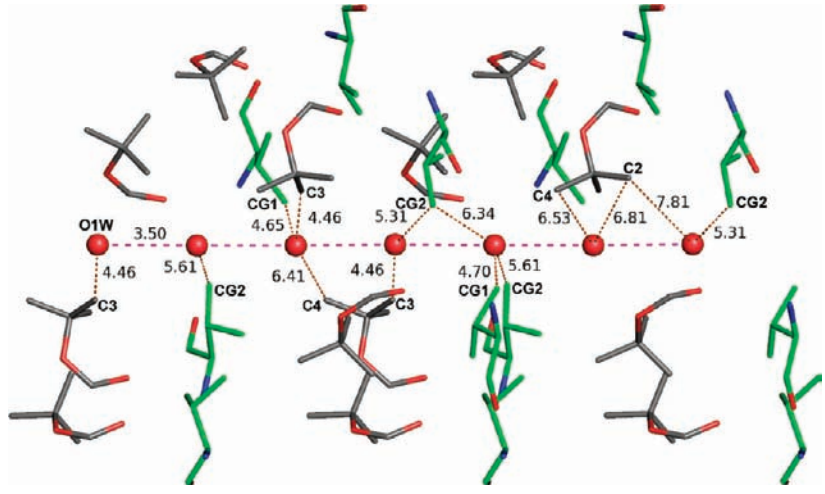

Figure 7. Model of a water wire inside the hydrophobic channel of the peptide **6a**, Boc-Pro-Aib-^{D}Val-Aib-^{D}Val-OMe. The residues lining the inner wall of the pore are shown as sticks (^{D}Val in green and Boc protecting group in gray). Crystallographically (space group $P6_1$) generated water molecules are shown as spheres. The hydrogen bonds between the water molecules are shown as dashed lines (magenta). Non-covalent weak interactions of the water oxygens with the peptide heavy atoms are also indicated as dots (orange). Distances marked are in angstroms.

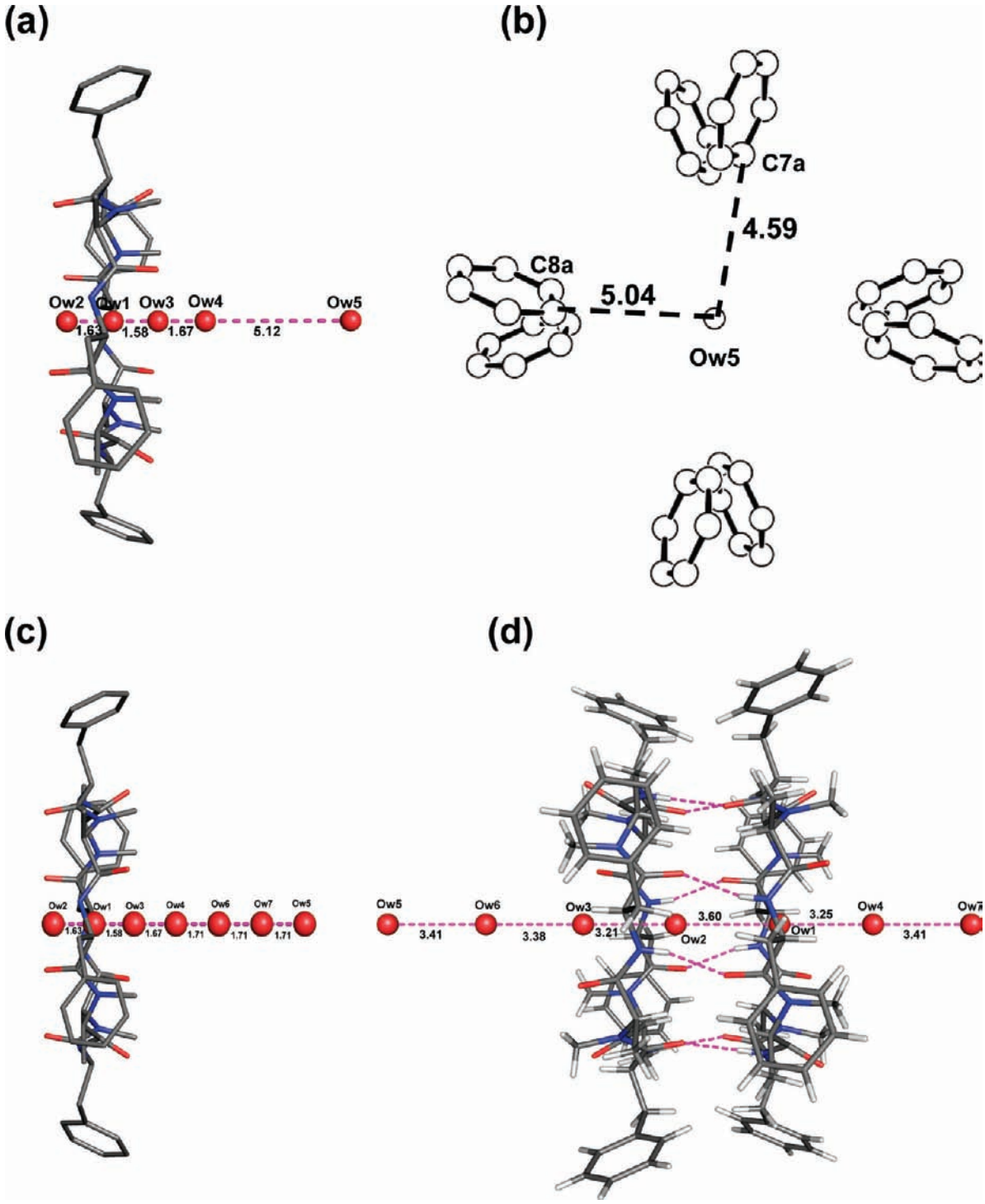

Figure 8. Cyclic peptide cyclo-[(Phe-^{D,Me}NAla)$_4$-](from ref 3c, redrawn using coordinates obtained from Cambridge Structure Database[22]). (a) Asymmetric unit as in the crystal structure, with five disordered water positions shown. (b) Environment of the water oxygen Ow5, revealing the zero-coordination. (c) Proposed structure with two additional oxygen atoms between Ow4 and Ow5. (d) Proposed water wire model inside the peptide. Distances between atoms are shown as dashed lines (magenta, values given in angstroms).

of single-file water wires to transport protons across narrow hydrophobic channels was first investigated by the multistate empirical valence bond method by Voth and co-workers.[14] These studies suggested that the rate of proton transport could be dramatically enhanced upon constricting a hydrophobic channel to dimensions where only a single-file water wire could be sterically accommodated. Molecular dynamics simulations have yielded valuable insights into the properties of water wires in apolar environments. In cavities of large dimensions, distinctive hydrogen-bonded clusters of water structures may be stabilized.[15] An intriguing recent report provides crystallographic support for novel structures for a hydrated proton inside a hydrophobic nanotube formed in crystals of a carborane acid.[16]

Clusters of water molecules have been found embedded within membrane-spanning segments of a number of channel-forming proteins. A particularly interesting example of this is

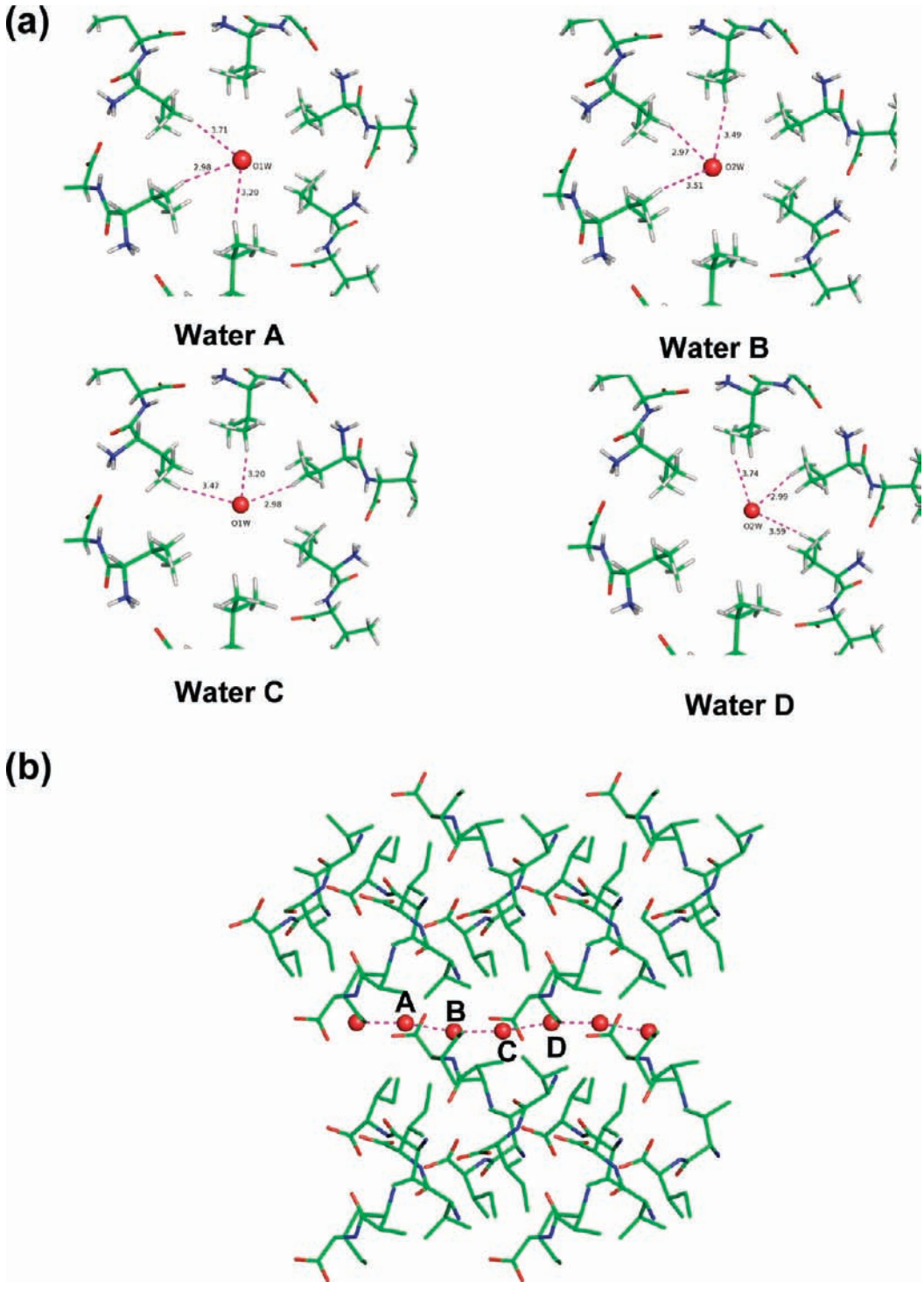

Figure 9. Linear dipeptide Val-Ile (from ref 4d, redrawn using coordinates obtained from Cambridge Structure Database[22]). (a) Environment of the four water molecules in the unit cell within the tubular peptide. The peptide atoms are shown as sticks. The shortest distances of the water oxygen with the atoms lining the pore interior are shown as dashed lines (magenta, values given in angstroms). (b) Modeled water wire inside the dipeptide Val-Ile.

the recent structure determination of the influenza virus proton channel, which is formed by the M2 protein.[17] The M2 channel has a relatively poor conduction rate of less than 10^4 protons/s, which is significantly lower than those of the other proton channels. The structural work suggests the absence of a large pore and does not provide evidence for a continuous water wire

(12) (a) Day, T. J. F.; Schmitt, U. W.; Voth, G. A. *J. Am. Chem. Soc.* **2000**, *122*, 12027–12028. (b) Ermler, U.; Fritzsche, G.; Buchanan, S. K.; Michel, H. *Structure* **1994**, *2*, 925–936. (c) Seibold, S. A.; Mills, D. A.; Ferguson-Miller, S.; Cukier, R. I. *Biochemistry* **2005**, *44*, 10475–10485. (d) Cui, Q.; Karplus, M. J. *J. Phys. Chem. B* **2003**, *107*, 1071–1078. (e) Lamoureux, G.; Klein, M. L.; Bernèche, S. *Biophys. J.* **2007**, *92*, L82–L84. (f) Luecke, H.; Schobert, B.; Richter, H. T.; Cartailler, J. P.; Lanyi, J. K. *J. Mol. Biol.* **1999**, *291*, 899–911.

(13) (a) Lu, D.; Voth, G. A. *J. Am. Chem. Soc.* **1998**, *120*, 4006–4014. (b) Voth, G. A. *Acc. Chem. Res.* **2006**, *39*, 143–150. (c) Swanson, J. M. J.; Maupin, C. M.; Chen, H.; Petersen, M. K.; Xu, J.; Wu, Y.; Voth, G. A. *J. Phys. Chem. B* **2007**, *111*, 4300–4314.

(14) Brewer, M. L.; Schmitt, U. W.; Voth, G. A. *Biophys. J.* **2001**, *80*, 1691–1702.

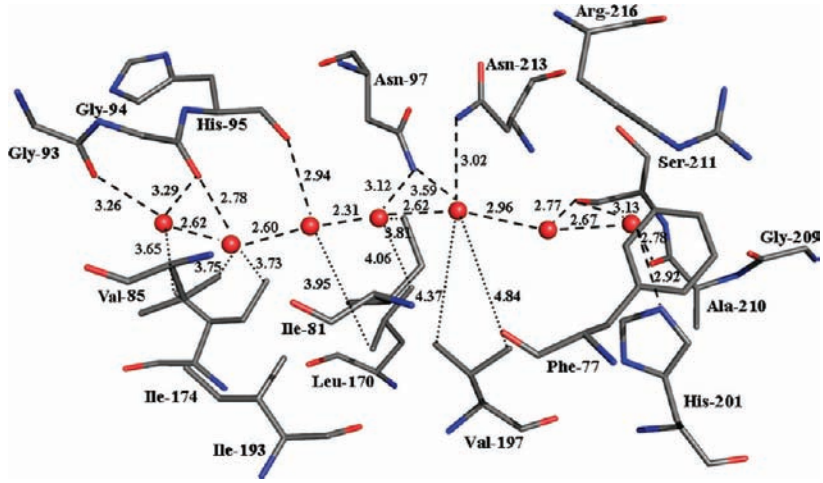

Figure 10. Experimentally observed single-file water inside the human aquaporin AQP4 (ref 11e, drawn using the cooordinate set PDB ID 3GD8 from the Protein Databank[23] using PyMol[24]). Shown in sticks are the residues forming the amphipathic faces of the water channel. The hydrogen-bonding distances between the water oxygens in the water wire and with the residues of the hydrophilic face are shown as dashed lines (distances given in Å). The distances of the water oxygens closest to the hydrophobic face of the channel are indicated as dotted lines.

spanning the membrane. Molecular dynamics studies of the M2 transmembrane domain provide evidence for water penetration deep into the transmembrane helix regions.[18] The infiltration of water molecules into the membrane channel specific for alkali cations has also been established in recent structural work on the NaK channel from *Bacillus cereus*.[19]

Conclusions

The water wires considered above consist of a one-dimensional assembly of water molecules which participate as a donor/acceptor in hydrogen bond interactions with preceding and succeeding water molecules. Two classes of O···O distances have been observed: 2.6−2.9 Å in the case of peptide **2a**, the dipeptide Val-Ile,[4c] and the human aquaporin AQP4[11e] and 3.2−3.5 Å in the case of peptides **2b**, **6a**, and cyclic peptide nanotubes reported by Ghadiri and co-workers.[3c] In the case of hydrophobic tubes, the second hydrogen atom points toward the walls of the tube, but in all cases discussed above, except the aquaporins, there does not appear to be any strong interaction involving this O−H bond. Tubular peptide channels considered above have diameters in the range 5.2−7.7 Å, with the water molecules aligned along the long axis of the tube. The absence of strong interactions with the walls of the tube in the case of peptide nanotubes would permit rapid rotation of water molecules about the axis of the tube. Such a motion must contribute to rotational entropy, which in turn may be a factor resulting in a lower overall free energy for the encapsulated water wire.[20] Rotational motion in a direction perpendicular to the tube axis should permit interchange of donor/acceptor interactions in a concerted fashion, providing a mechanism for Grotthuss-type proton transport, which has been favored as a mechanism for proton conduction in ordered water arrays.[12,14,20,21] In contrast, the architecture of the aquaporin water channels anchors the second O−H bond of the water molecule in a strong hydrogen bond interaction with the polar side chains which line the channel.[11e] Water hops between hydrogen-bonding sites may then be a mechanism for the single-file transport through the protein pores. The two crystal forms of peptide **2** (**2a** and **2b**) characterized earlier provided an example of both short hydrogen bond ($d_{O\cdots O}$ = 2.6 Å) and long hydrogen bond ($d_{O\cdots O}$ = 3.5 Å) arrangements of the water wires. The latter was obtained by the transformation of the originally formed crystals. Peptide **2** and its enantiomorph **6** present examples of multiple crystal forms, and different packing arrangements could be obtained. The structure of peptide **6a** reveals a porous lattice with water

(15) (a) Blanton, W. B. B.; Gordon-Wylie, S. W.; Clark, G. R.; Jordan, K. D.; Wood, J. T.; Geiser, U.; Collins, T. J. *J. Am. Chem. Soc.* **1999**, *121*, 3551–3552. (b) Barbour, L. J.; Orr, G. W.; Atwood, J. L. *Chem. Commun.* **2000**, 859–860. (c) Custelcean, R.; Afloroaei, C.; Vlassa, M.; Polverejan, M. *Angew. Chem., Int. Ed.* **2000**, *39*, 3094–3096. (d) Moorthy, J. N.; Natarajan, R.; Venugopalan, P. *Angew. Chem., Int. Ed.* **2002**, *41*, 3417–3420. (e) Doedens, R. J.; Yohannes, E.; Khan, M. I. *Chem. Commun.* **2002**, 62–63. (f) Pal, S.; Sankaran, N. B.; Samanta, A. *Angew. Chem., Int. Ed.* **2003**, *42*, 1741–1743. (g) Ghosh, S. K.; Bharadwaj, P. K. *Inorg. Chem.* **2003**, *42*, 8250–8254. (h) Ma, B.; Sun, H.; Gao, S. *Angew. Chem., Int. Ed.* **2004**, *43*, 1374–1376. Byl, O.; Liu, J.-C.; Wang, Y.; Yim, W. L.; Johnson, J. K.; Yates, J. T., Jr. *J. Am. Chem. Soc.* **2006**, *128*, 12090–12097. Mascal, M.; Infantes, L.; Chisholm, J. *Angew. Chem., Int. Ed.* **2006**, *45*, 32–36.
(16) Stoyanov, E. S.; Stoyanova, I. V.; Tham, F. S.; Reed, C. A. *J. Am. Chem. Soc.* **2009**, *131*, 17540–15441.
(17) Stoufer, A. L.; Acharya, R.; Salom, D.; Levine, A. S.; Costanzo, D. L.; Soto, C. S.; Tereshko, V.; Nanda, V.; Stayrook, S.; DeGrado, W. F. *Nature* **2008**, *451*, 596–600.
(18) (a) Yi, M.; Cross, T. A.; Zhou, H. X. *Proc. Natl. Acad. Sci. U.S.A.* **2009**, *106*, 13311–13316. (b) Khurana, E.; Peraro, M. D.; DeVane, R.; Vemparala, S.; DeGrado, W. F.; Klein, M. L. *Proc. Natl. Acad. Sci. U.S.A.* **2009**, *106*, 1069–1074.
(19) (a) Alam, A.; Jiang, Y. *Nat. Struct. Mol. Biol.* **2009**, *16*, 30–34. (b) Alam, A.; Jiang, Y. *Nat. Struct. Mol. Biol.* **2009**, *16*, 35–41.
(20) (a) Pomes, R.; Roux, B. *Biophys. J.* **1996**, *71*, 19–39. (b) Hummer, G.; Rasaiah, J. C.; Noworyta, J. P. *Nature* **2001**, *414*, 188–190. (c) Berezhkovskii, A.; Hummer, G. *Phys. Rev. Lett.* **2002**, 89064503.
(21) (a) Agmon, N. *Chem. Phys. Lett.* **1995**, *244*, 456–462. (b) Pomes, R.; Roux, B. *Biophys. J.* **2002**, *82*, 2304–2316. (c) Tajkhorshid, E.; Nollert, P.; Jensen, M. A.; Miercke, L. J. W.; O'Connell, J.; Stroud, R. M.; Schulten, K. *Science* **2002**, *296*, 525–530. (d) Burykin, A.; Warshel, A. *Biophys. J.* **2003**, *85*, 3696–3706. (e) Chakrabarti, N.; Tajkhorshid, E.; Roux, B.; Pomes, R. *Structure* **2004**, *12*, 65–74. (f) Dellago, C.; Hummer, G. *Phys. Rev. Lett.* **2006**, *97*, 245901. (g) Takhashi, R.; Wang, H.; Lewis, J. P. *J. Phys. Chem. B* **2007**, *111*, 9093–9098. (h) Alexiadis, A.; Kassinos, S. *Chem. Rev.* **2008**, *108*, 5014–5034. (i) Kofinger, J.; Hummer, G.; Dellago, C. *Proc. Natl. Acad. Sci. U.S.A.* **2008**, *105*, 13218–13222. (j) Parthasarathi, R.; Elango, M.; Subramanian, V.; Sathyamurthy, N. *J. Phys. Chem. A* **2009**, *113*, 3744–3749.
(22) Allen, F. H. *Acta Crystallogr., Sect. C* **2002**, *58*, 380–388.
(23) Bernstein, F. C.; Koetzle, T. F.; Williams, G. J.; Meyer, E. E., Jr.; Brice, M. D.; Rodgers, J. R.; Kennard, O.; Shimanouchi, T.; Tasumi, M. *J. Mol. Biol.* **1977**, *112*, 535.
(24) DeLano, W. L. *The PyMOL Molecular Graphics System*; DeLano Scientific LLC: San Carlos, CA, 2002; http://www.pymol.org.

entrapped within hydrophobic channels, while **6b** crystallizes in a monoclinic form in a close-packed arrangement. In contrast, we have thus far been able to obtain only one crystal form which contains empty hydrophobic channels. In the case of peptide **1** and the enantiomorph **5**, the side chains of isobutyl groups project inside the channel interior, thereby limiting the diameter of the pore. Close-packed structures are formed when the projecting side chains are reduced in size, as in the case of peptide **3** (Xxx = Ala) and the enantiomorph **6** (^{D}Xxx = ^{D}Ala), or increased, as in the case of peptide **4** (Xxx = Phe) and the enantiomorph **8** (^{D}Xxx = ^{D}Phe). Water-filled pores have thus far been characterized only in the case of projecting isopropyl side chains for the Val residue in the peptides **2** and **6**. Further characterization of the water structures inside the hydrophobic tubes may provide additional insights into the properties of water wires. The incorporation of other guest molecules and further tuning of the channel diameter and properties of the walls using modified amino acids remains to be explored.

Experimental Section

The peptides for the studies were synthesized by solution-phase procedures using a racemization-free fragment condensation strategy. The *tert*-butoxycarbonyl (Boc) group was used for *N*-terminal protection, and the *C*-terminal was protected as a methyl ester. The Boc deprotection was performed using 98% formic acid and methyl ester by saponification. The final step in the synthesis of peptides was achieved by the fragment condensation of Boc-^{D}Pro-OH/Boc-Pro-OH with H_2N-Aib-Xxx-Aib-Val-OMe (Xxx = Leu, Val, Ala, Phe, and its D-isomers) using *N*,*N*′-dicyclohexylcarbodiimide (DCC)/1-hydroxybenzotriazole (HOBt) as the coupling reagent. All the intermediates were characterized by electrospray ionization mass spectrometry (ESI-MS) on a Bruker Daltonics Esquire-3000 instrument and thin-layer chromatography (TLC) on silica gel and used as such for the final step. The final peptides were purified by reverse-phase medium-pressure liquid chromatography (RP-MPLC, C_{18}, 40−60 μm) and high-performance liquid chromatography (HPLC) on a reverse-phase C_{18} column (5−10 μm, 7.8 mm × 250 mm) using methanol/water gradients. The purified peptides were characterized by ESI-MS. Mass spectral data (*m*/*z*): peptides **1** and **5**, 612.2 $[M + H]^+$ (M_{cal} = 611.4 Da), 634.2 $[M + Na]^+$, 650.5 $[M + K]^+$; **2** and **6**, 598.5 $[M + H]^+$ (M_{cal} = 597.4 Da), 620.5 $[M + Na]^+$, 636.2 $[M + K]^+$; **3** and **7**, 570.4 $[M + H]^+$ (M_{cal} = 569.3 Da), 592.2 $[M + Na]^+$; **4** and **8**, 646.4 $[M + H]^+$ (M_{cal} = 645.4 Da); 668.4 $[M + Na]^+$, 684.4 $[M + K]^+$.

Colorless crystals were grown by the slow evaporation method for peptides **1**−**8**. The crystals of **1**, **3**, **6b**, and **7** were grown from methanol solution, to which a small amount of water was added. Peptide crystals for **2** and **6a** were obtained from a mixture of ethyl acetate/petroleum ether. Crystals for **4** were grown from a mixture of acetonitrile/water, and those of **5** and **8** were obtained from a solution in dioxane, to which a small amount of water was added. The X-ray diffraction data collected for the crystals of **1**−**8** are summarized in Table 1 (see Supporting Information for details). The structures were solved by direct methods using SHELXS-97 and refined against F^2, with full-matrix least-squares methods by using SHELXL-97. The final values after the refinement of crystal structures are shown in the Table 1 (see Supporting Information Tables S1−S6 for details).

Acknowledgment. This work is supported by a grant from the Council of Scientific and Industrial Research (CSIR), India and a program grant from the Department of Biotechnology (DBT), India, in the area of Molecular Diversity and Design. U.S.R. and S.A. thank the University Grants Commission and CSIR, India, for a Senior Research Fellowship and Research Associateship, respectively. Kantharaju is supported by the award of a DBT Postdoctoral Fellowship from the DBT, India. X-ray diffraction data were collected at the CCD facility under IRHPA program of the Department of Science and Technology, India and by the Indian Institute of Science, Bangalore, India.

Supporting Information Available: X-ray crystallographic characterization details (Tables S1−S6) and CIF files for **1**, **2a**, **2b**, **3**, **4**, **5**, **6a**, and **6b**. This material is available free of charge via the Internet at http://pubs.acs.org. CCDC deposition numbers for peptides are 728333 (**1**), 728334 (**2a**), 728335 (**2b**), 749313 (**3**), 749314 (**4**), 749317 (**5**), 749318 (**6a**), 749319 (**6b**), 749315 (**7**), and 749316 (**8**).

JA9083978